PHYSICAL REVIEW D **90,** 096008 (2014)

Chiral symmetry and π-π scattering in the covariant spectator theory

Elmar P. Biernat,[1,*] M. T. Peña,[1,2,†] J. E. Ribeiro,[3,‡] Alfred Stadler,[4,1,§] and Franz Gross[5,∥]

[1]Centro de Física Teórica de Partículas (CFTP), Instituto Superior Técnico (IST), Universidade de Lisboa, 1049-001 Lisboa, Portugal

[2]Departamento de Física, Instituto Superior Técnico (IST), Universidade de Lisboa, 1049-001 Lisboa, Portugal

[3]Centro de Física das Interações Fundamentais (CFIF), Instituto Superior Técnico (IST), Universidade de Lisboa, 1049-001 Lisboa, Portugal

[4]Departamento de Física, Universidade de Évora, 7000-671 Évora, Portugal

[5]Thomas Jefferson National Accelerator Facility (JLab), Newport News, Virginia 23606, USA

(Received 5 August 2014; published 14 November 2014)

The π-π scattering amplitude calculated with a model for the quark-antiquark interaction in the framework of the covariant spectator theory (CST) is shown to satisfy the Adler zero constraint imposed by chiral symmetry. The CST formalism is established in Minkowski space and our calculations are performed in momentum space. We prove that the axial-vector Ward-Takahashi identity is satisfied by our model. Then we show that, similar to what happens within the Bethe-Salpeter formalism, application of the axial-vector Ward-Takahashi identity to the CST π-π scattering amplitude allows us to sum the intermediate quark-quark interactions to all orders. The Adler self-consistency zero for π-π scattering in the chiral limit emerges as the result for this sum.

DOI: 10.1103/PhysRevD.90.096008 PACS numbers: 11.30.Rd, 12.38.Lg, 12.39.Pn, 14.40.Be

I. INTRODUCTION

In the present scenario of both experimental and theoretical hadron physics the pion remains an important system to trace signatures of QCD in empirical observables. The importance of the pion is multifaceted: it emerges nonperturbatively as a quark-antiquark bound state, it is the Goldstone-boson mode associated with spontaneous chiral-symmetry breaking (SχSB), and it also contributes significantly, through the formation of a pion cloud, to the structure of the nucleon and to its coupling to external photons. In addition, the exchange of pions dominates the interaction between nucleons at larger distances and gives rise to a tensor force that strongly influences the structure of nuclei.

Traditionally, the nonperturbative dynamics underlying hadronic systems have been addressed from two different perspectives, constituent quark models [1–4] and QCD sum rules. These approaches, however, cannot provide a unified description of light mesons and baryons, nor can they avoid a delicate fine-tuning between a large number of parameters. More recently, QCD simulations on the lattice [5,6], light-front formulations of quantum field theory [7–9], as well as models based on the Dyson-Schwinger approach and mass gap equation [10–20] have contributed to a more integrated perspective of mesons and baryons.

In particular, the Dyson-Schwinger framework generates dynamical quark models where the dressed quark mass is calculated as a function of the momentum, and moreover, this dynamical generation of quark masses is made consistent with the two-body quark-antiquark dynamics. However, lattice QCD and Dyson-Schwinger equations are usually solved in Euclidean space. In contrast, the covariant spectator theory (CST), used in this paper, works in Minkowski space, and also exhibits these features.

First model calculations of the pion form factor using the solutions of the CST-Bethe-Salpeter equation (CST-BSE) and the CST-Dyson equation (CST-DE) were presented in Ref. [21]. There, the CST interaction kernel in momentum space was taken as a δ function *plus* a covariant generalization of the linear confining interaction.

The confining part in momentum space contains an important subtraction term that makes sure that it reduces to the linear potential (in coordinate space) $V_L(r) \propto r$ in the nonrelativistic limit. In particular, it was seen in Ref. [22] that the condition $V_L(r=0) = 0$ implies that the confinement interaction decouples from the CST-DE for the scalar part of the dressed quark propagator, as well as from the CST-BSE for a massless pion in the chiral limit. For a scalar confining interaction, this decoupling property of our CST model is a necessary condition to ensure consistency with chiral symmetry. For the numerical predictions, our model was calibrated by adjusting the dressed quark mass function to the existing lattice QCD data.

In this paper we submit our model to a more stringent test. We present the CST calculation of the π-π scattering amplitude in the chiral limit, and conclude that it satisfies

*elmar.biernat@tecnico.ulisboa.pt
†teresa.pena@tecnico.ulisboa.pt
‡emilioribeiro@tecnico.ulisboa.pt
§stadler@uevora.pt
∥gross@jlab.org

the Adler self-consistency zero as imposed by chiral symmetry (see Ref. [23]), provided the interaction kernel satisfies the axial-vector Ward-Takahashi identity (AV-WTI). There are various possible choices for the Lorentz structure of the kernel that satisfy the AV-WTI. We choose a mixture of scalar, pseudoscalar, vector, axial-vector, and tensor structures for the confining interaction, in combination with a vector–axial-vector structure for the remaining part of the kernel. Although one lacks first-principle evidence for scalar quark confinement, it is still quite important to study to what extent such confining forces can be made compliant with SχSB. To this effect the AV-WTI will play a fundamental role when it comes to evaluate, to all orders of kernel insertions and independently of parameter fixing, π-π scattering and the corresponding π-π Adler zero.

This paper is organized as follows: In Sec. II a brief review of the CST formalism is given. In Sec. III we discuss the constraints imposed by the AV-WTI on the CST interaction kernel and we specify the particular form of the kernel to be used in this paper. In Sec. IV we present a calculation of π-π scattering, first in the simple impulse approximation that is seen not to comply with the Adler zero in the chiral limit, and then to all orders in intermediate interactions that does yield the Adler zero. Finally, in Sec. V we present a brief summary and our main conclusions.

II. BRIEF REVIEW OF THE CST FRAMEWORK

The purpose of this section is to briefly review the basic ideas of the CST when applied to quark-antiquark mesons [24,25]. First, let us consider the four-dimensional BSE [26] for heavy-light mesons. It is well known [27] that cancellations occur between iterations of ladder diagrams and higher-order crossed-ladder diagrams in the complete kernel of the BSE. Owing to this, the omission of crossed-ladder diagrams and of certain pole contributions of the ladder diagrams from the kernel can actually yield a better approximation to the exact BSE than the ladder approximation does.

This fundamental idea of CST emerges more formally from reorganizing the Bethe-Salpeter series, with a complete kernel and (off-mass-shell) two-particle propagators, into an equivalent form—the CST equation—where *both* the kernel and propagators in the intermediate states are redefined. In the heavy-light case, the new quark propagators are chosen in such a way that, when the new kernel is truncated, only the positive-energy pole contribution from the heavy quark propagator in the energy loop integration is kept, which effectively corresponds to taking the heavy quark to be on its positive-energy mass shell.

The resulting three-dimensional equation, the one-channel CST (or Gross) equation [28], is manifestly covariant. But, unlike the BSE in ladder approximation, the CST equation also has a smooth nonrelativistic limit, and it can thus be viewed as a natural covariant extension of the quantum mechanical Dirac and Schrödinger equations to quantum field theory. While the simple CST equation is very efficient for the description of heavy-light mesons, in the case of light quarks an explicitly charge-conjugation-symmetrized CST-BSE must be used. This is the case for the pion where the vertex functions of π^+ and π^- are connected by charge conjugation and, therefore, both positive- and negative-energy quark poles must be included.

The idea of symmetrizing over all quark poles generates the charge-conjugation-symmetric CST-BSE [25],

$$\begin{aligned}\Gamma(p_1,p_2) = &-\frac{1}{2}Z_0\int_k\bigg[\mathcal{V}\Big(p,\hat{k}-\frac{1}{2}P\Big)\Lambda(\hat{k})\Gamma(\hat{k},\hat{k}-P)S(\hat{k}-P)+\mathcal{V}\Big(p,\hat{k}+\frac{1}{2}P\Big)S(\hat{k}+P)\Gamma(\hat{k}+P,\hat{k})\Lambda(\hat{k})\\ &+\mathcal{V}\Big(p,-\hat{k}-\frac{1}{2}P\Big)\Lambda(-\hat{k})\Gamma(-\hat{k},-\hat{k}-P)S(-\hat{k}-P)+\mathcal{V}\Big(p,-\hat{k}+\frac{1}{2}P\Big)S(-\hat{k}+P)\Gamma(-\hat{k}+P,-\hat{k})\Lambda(-\hat{k})\bigg]\\ \equiv{}& \mathrm{i}\int_{k0}\mathcal{V}(p,k)S\Big(k+\frac{P}{2}\Big)\Gamma\Big(k+\frac{P}{2},k-\frac{P}{2}\Big)S\Big(k-\frac{P}{2}\Big),\end{aligned} \tag{1}$$

where we use the shorthand notation for the three-dimensional covariant integration volume element,

$$\int_k \equiv \int\frac{\mathrm{d}^3k}{(2\pi)^3}\frac{m}{E_k}, \tag{2}$$

and the last line of Eq. (1) introduces the notation "$k0$" to indicate the charge-conjugation invariant CST prescription for performing the k_0 contour integration. This amounts to keeping the average of the four propagator pole contributions from closing the contour in both the upper and the lower half-complex k_0 plane (for more details see Ref. [25]). With these definitions,

$$\mathrm{i}\int_{k0} \equiv \mathrm{i}\int\frac{\mathrm{d}^4k}{(2\pi)^4}\bigg|_{k_0\text{ propagator poles only}} = -\frac{1}{2}\sum_{\substack{\text{propagator}\\ \text{pole terms}}}\int_k. \tag{3}$$

The quantities in Eq. (1) are $\Gamma(p_1,p_2)$, the (4×4) bound-state vertex function with $p_1 = p+\frac{P}{2}$ and $-p_2 = -p+\frac{P}{2}$ the four-momenta of the outgoing quark and antiquark (respectively); P, the total bound-state momentum; $\hat{k} = (E_k, \mathbf{k})$, the on-shell four-momentum with $E_k = \sqrt{m^2 + \mathbf{k}^2}$; $\mathcal{V}(p,k) \equiv \mathcal{V}(p,k;P)$, the interaction kernel; $S(k)$, the dressed quark propagator; and $\Lambda(k) = [M(k^2) + \not{k}]/2M(k^2)$, where $M(k^2)$ is the dressed quark mass function. The kernel is an operator, and we use the shorthand notation

$$\mathcal{V}(p,k)\mathcal{X} \equiv \sum_i V_i(p,k)\mathcal{O}_i \mathcal{X} \mathcal{O}_i, \tag{4}$$

where the sum $i = \{S, P, V, A, T\}$ is over the five possible invariant structures that could contribute: scalar, pseudoscalar, vector, axial-vector, and tensor. This will be discussed further when it is needed below. The dressed quark propagator is given by

$$S(p) = \frac{1}{m_0 - \not{p} + \Sigma(p) - \mathrm{i}\epsilon}, \tag{5}$$

where m_0 is the bare quark mass and $\Sigma(p)$ is the quark self-energy, which is the solution of the one-body CST-DE involving, for consistency, the *same* interaction kernel $\mathcal{V}$ that dresses the quark-antiquark vertex. The CST-DE is given by [25]

$$\Sigma(p) = \frac{1}{2} Z_0 \int_k \{\mathcal{V}(p,\hat{k})\Lambda(\hat{k}) + \mathcal{V}(p,-\hat{k})\Lambda(-\hat{k})\}$$
$$\equiv -\mathrm{i}\int_{k0} \mathcal{V}(p,k)S(k). \tag{6}$$

Writing the self-energy in the form

$$\Sigma(p) = A(p^2) + \not{p}B(p^2) \tag{7}$$

leads to a dressed propagator of the form

$$S(p) = Z(p^2)\frac{M(p^2) + \not{p}}{M^2(p^2) - p^2 - \mathrm{i}\epsilon}, \tag{8}$$

where the mass function $M(p^2)$ and the wave function normalization $Z(p^2)$ are

$$M(p^2) = \frac{A(p^2) + m_0}{1 - B(p^2)},$$
$$Z(p^2) = \frac{1}{1 - B(p^2)}, \tag{9}$$

and $Z_0 \equiv Z(m^2)$. For $\Sigma(p) = 0$, $S(p)$ becomes the bare propagator denoted as $S_0(p)$.

A proof of principle that the CST-Bethe-Salpeter equation (1) and the CST-Dyson equation (6) are actually numerically manageable in Minkowski space and that they underlie a dynamical quark model that incorporates SχSB (similar to the Dyson-Schwinger approach) was presented in Refs. [21,25]. In this paper we build on the model introduced in those recent references, where technical details can be found.

It was already proven in Refs. [25,29] that in the chiral limit the pion mass also vanishes, which means that the CST equations are, at least at this level, not inconsistent with the requirements of dynamical chiral symmetry breaking. In the present work we look at the implications of chiral symmetry on our model coming from the AV-WTI and π-π scattering in the chiral limit.

III. THE AXIAL-VECTOR WARD-TAKAHASHI IDENTITY AND THE INTERACTION KERNEL

A. The axial-vector Ward-Takahashi identity

In our previous work, Ref. [25], the quark-antiquark interaction was regularized by a strong quark form factor h associated with each quark line entering or leaving a vertex. These form factors can be moved from the interaction vertices to the quark propagators, which leads to the replacement of the original kernel $\mathcal{V}(p,k)$ by a reduced kernel $\mathcal{V}_R(p,k)$, dressed propagators $S(p)$ by damped dressed propagators $\tilde{S}(p) = h^2(p^2)S(p)$, and bare propagators $S_0(p)$ by damped bare propagators $\tilde{S}_0(p) = h^2(p^2)S_0(p)$. We use reduced kernels that depend only on the square of the transferred momentum, such that

$$\mathcal{V}_R(p-k) = h^{-1}(p^2)h^{-1}(p'^2)h^{-1}(k^2)h^{-1}(k'^2)\mathcal{V}(p,k), \tag{10}$$

where $\mathcal{V}(p,k)$ is the kernel of Eq. (1).

Chiral symmetry and its breaking is expressed through the AV-WTI, which can be derived from the divergence of the axial-vector current [30]. Expressed in terms of the reduced vertex functions and the damped propagators, the familiar AV-WTI for off-shell quarks is

$$P_\mu \Gamma_R^{5\mu}(p',p) + 2m_0\Gamma_R^5(p',p) = \tilde{S}^{-1}(p')\gamma^5 + \gamma^5\tilde{S}^{-1}(p)$$
$$\equiv \Gamma_R^A(p',p), \tag{11}$$

where $\Gamma_R^{5\mu}(p',p)$ is the reduced dressed axial-vector vertex, $\Gamma_R^5(p',p)$ the reduced dressed pseudoscalar vertex, $\tilde{S}(p)$ the damped dressed propagator, p and p' are the incoming and outgoing quark momenta, respectively, and $P = p' - p$ is the momentum flowing into the vertex to which the incoming and outgoing quarks connect. The quantity $\Gamma_R^A(p',p)$ defined by the lhs of Eq. (11), which we refer to as the "axial vertex," is a convenient combination of the axial-vector and the pseudoscalar vertices used in Refs. [31,32]. The identity (11) is illustrated in the upper panel of Fig. 1. Note that the AV-WTI for bare quark propagators S_0 implies that the bare axial-vector and pseudoscalar vertices are $\gamma^5\gamma^\mu$ and γ^5, respectively.

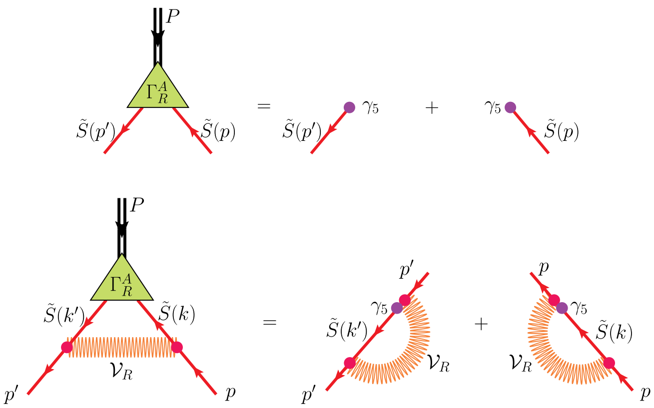

FIG. 1 (color online). (Top panel) The AV-WTI illustrated diagrammatically for the dressed current. (Bottom panel) Representation of the rhs of Eq. (12) after application of the AV-WTI from the top panel. Each red arrowed line denotes a dressed quark propagator. The purple blobs denote γ^5 matrices and the pink blobs denote the Dirac structure of the kernel.

The dressed axial-vector vertex, the dressed pseudoscalar vertex, and the dressed axial vertex, $\Gamma_R^A(p',p)$, are all solutions of an inhomogeneous CST-BSE. For the axial vertex,

$$\Gamma_R^A(p',p) = \gamma_R^A(p',p) + \mathrm{i}\int_{k0} \mathcal{V}_R(p-k)\tilde{S}(k')\Gamma_R^A(k',k)\tilde{S}(k), \tag{12}$$

where $\gamma_R^A(p',p)$ is the reduced bare axial vertex (to be discussed below) and Eq. (12) is depicted diagrammatically in Fig. 2. Note that $p-k=p'-k'$. The dressed damped propagator $\tilde{S}(p)$ is the solution of the CST-DE

$$\tilde{S}^{-1}(p) = \tilde{S}_0^{-1}(p) - \mathrm{i}\int_{k0} \mathcal{V}_R(p-k)\tilde{S}(k). \tag{13}$$

Next, look at the implications of the AV-WTI (11) and how it relates to the one-body CST-DE (13) and to the inhomogeneous two-body CST-BSE (12). Using Eq. (11) in the integrand of Eq. (12), the result splits into two terms,

$$\begin{aligned}\Gamma_R^A(p',p) &= \gamma_R^A(p',p) + \mathrm{i}\int_{k0} \mathcal{V}_R(p-k)\tilde{S}(k') \\ &\quad\times [\tilde{S}^{-1}(k')\gamma^5 + \gamma^5\tilde{S}^{-1}(k)]\tilde{S}(k) \\ &= \gamma_R^A(p',p) + \mathrm{i}\int_{k0} \mathcal{V}_R(p-k)\gamma^5\tilde{S}(k) \\ &\quad + \mathrm{i}\int_{k0} \mathcal{V}_R(p'-k')\tilde{S}(k')\gamma^5,\end{aligned} \tag{14}$$

where $p'=P+p$ and $k'=P+k$, as illustrated in the lower panel of Fig. 1. On the other hand, with the shorthand notation $h=h(p^2)$ and $h'=h(p'^2)$, the rhs of Eq. (11) reads

$$\begin{aligned}&\frac{m_0-\not{p}'+\Sigma(p')}{h'^2}\gamma_5+\gamma_5\frac{m_0-\not{p}+\Sigma(p)}{h^2} \\ &\quad= \gamma^5\left[\frac{\not{p}'}{h'^2}-\frac{\not{p}}{h^2}\right]+m_0\left[\frac{1}{h'^2}+\frac{1}{h^2}\right]\gamma_5+\frac{\Sigma(p')}{h'^2}\gamma_5+\gamma_5\frac{\Sigma(p)}{h^2},\end{aligned} \tag{15}$$

and we can now compare Eq. (14) with (15).

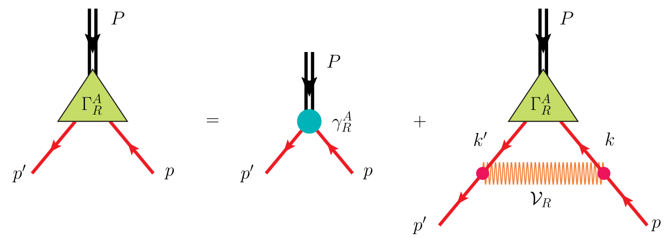

FIG. 2 (color online). The inhomogeneous CST-BSE for $\Gamma_R^A(p',p)$.

B. The reduced bare vertex

First, on both sides we identify all quantities that do not involve contributions to the self-energy from the dynamical dressing by the kernel, and conclude that

$$\begin{aligned}\gamma_R^A(p',p) &= \gamma_5\left[\frac{\not{p}'}{h'^2}-\frac{\not{p}}{h^2}\right]+m_0\left[\frac{1}{h'^2}+\frac{1}{h^2}\right]\gamma_5 \\ &= \tilde{S}_0^{-1}(p')\gamma^5+\gamma^5\tilde{S}_0^{-1}(p).\end{aligned} \tag{16}$$

This is an AV-WTI for the damped bare vertex and propagators. It can be satisfied by decomposing $\gamma_R^A(p',p)$ into its pseudoscalar and axial-vector parts,

$$\gamma_R^A(p',p) = P_\mu\gamma_R^{5\mu}(p',p)+2m_0\gamma_R^5(p',p), \tag{17}$$

and making the following simple *Ansätze* for $\gamma_R^{\mu5}$ and γ_R^5 in the manner of Refs. [33–35]:

$$\begin{aligned}\gamma_R^{5\mu}(p',p) &= f_A(p',p)\gamma^5\gamma^\mu \\ &\quad+ g_A(p',p)\Lambda_0(-p')\gamma^5\gamma^\mu\Lambda_0(-p)\end{aligned} \tag{18}$$

and

$$\begin{aligned}\gamma_R^5(p',p) &= f_P(p',p)\gamma^5 \\ &\quad+ g_P(p',p)\Lambda_0(-p')\gamma^5\Lambda_0(-p),\end{aligned} \tag{19}$$

where $\Lambda_0(p)=(m_0+\not{p})/2m_0$. The form factors $f_A(p',p)$, $g_A(p',p)$, $f_P(p',p)$, and $g_P(p',p)$ are then determined to be

$$f_A(p',p) = f_P(p',p) = \frac{m_0^2 - p'^2}{h'^2(p^2 - p'^2)} - \frac{m_0^2 - p^2}{h^2(p^2 - p'^2)} \tag{20}$$

$$g_A(p',p) = -g_P(p',p) = \frac{4m_0^2}{p'^2 - p^2}\left(\frac{1}{h^2} - \frac{1}{h'^2}\right). \tag{21}$$

If we set all quark form factors h to 1, then $f_A(p',p) \to 1$ and $g_A(p',p) \to 0$, such that $\gamma_R^{5\mu}(p',p) \to \gamma^5\gamma^\mu$ and $\gamma_R^5(p',p) \to \gamma^5$. In this case, the damped bare AV-WTI (16) becomes the bare one involving S_0, as used, for instance, in Ref. [32].

C. Constraints on the interaction kernel

The aim of this subsection is to determine the general form of the covariant interaction kernel $\mathcal{V}_R(p-k)$ such that the AV-WTI (11) is satisfied. Recalling the decomposition (4), the reduced kernel will be written in the form

$$\begin{aligned}\mathcal{V}_R(p-k) = {} & V_{SR}(p-k)\mathbf{1}\otimes\mathbf{1} + V_{PR}(p-k)\gamma^5\otimes\gamma^5 \\ & + V_{VR}(p-k)\gamma^\mu\otimes\gamma_\mu \\ & + V_{AR}(p-k)\gamma^5\gamma^\mu\otimes\gamma^5\gamma_\mu \\ & + \frac{1}{2}V_{TR}(p-k)\sigma^{\mu\nu}\otimes\sigma_{\mu\nu},\end{aligned} \tag{22}$$

where the corresponding factors in the decomposition of $\mathcal{V}(p,k;P)$ include the strong quark form factors and are therefore $V_i(p,p';k,k') = h(p^2)h(p'^2)h(k^2)h(k'^2)$ $V_{iR}(p-k)$. Using this decomposition, comparing Eqs. (14) and (15), and extracting the γ^5, we see that preserving the AV-WTI is tantamount to requiring that

$$\mathrm{i}\int_{k0}\hat{\mathcal{V}}_R(p-k)\tilde{S}(k) = \frac{\Sigma(p)}{h^2(p^2)}, \tag{23}$$

where the operator $\hat{\mathcal{V}}_R(p-k)$ is obtained from the operator $\mathcal{V}_R(p-k)$ by changing the sign of the vector and axial-vector components of $\mathcal{V}_R(p-k)$. Using (22), (23) reduces to

$$\begin{aligned}\frac{\Sigma(p)}{h^2(p^2)} = \mathrm{i}\int_{k0}\Big[& V_{SR}(p-k)\tilde{S}(k) + V_{PR}(p-k)\gamma^5\tilde{S}(k)\gamma^5 \\ & - V_{VR}(p-k)\gamma^\mu\tilde{S}(k)\gamma_\mu - V_{AR}(p-k)\gamma^5\gamma^\mu\tilde{S}(k)\gamma^5\gamma_\mu \\ & + \frac{1}{2}V_{TR}(p-k)\sigma^{\mu\nu}\tilde{S}(k)\sigma_{\mu\nu}\Big].\end{aligned} \tag{24}$$

By comparing this equation with the one-body CST-DE for the self-energy, Eq. (6), using the same kernel we conclude, given the signs in front of the scalar, pseudoscalar, and tensor interaction terms in (24), that the AV-WTI links the one-body CST-DE with the two-body CST-BSE, Eq. (14), if and only if

$$\begin{aligned}\int_{k0}\Big[& V_{SR}(p-k)\tilde{S}(k) + V_{PR}(p-k)\tilde{S}(-k) \\ & + \frac{1}{2}V_{TR}(p-k)\sigma^{\mu\nu}\tilde{S}(k)\sigma_{\mu\nu}\Big] = 0.\end{aligned} \tag{25}$$

In the literature, the most common realization of this type of condition is achieved by setting $V_{SR}(p-k) = V_{PR}(p-k) = V_{TR}(p-k) = 0$, i.e., by using only interaction kernels that anticommute with γ^5, like vector or axial-vector (e.g., see Refs. [32,36,37]).

In this work we use a kernel that *does* include nonvanishing scalar, pseudoscalar, and tensor structures, but is, nevertheless, consistent with the AV-WTI. Other models with this feature exist in the literature. In Ref. [38], a tensor term was chosen in such a way that Eq. (25) is satisfied. In our case, it is the implementation of linear confinement in the CST framework that makes sure Eq. (25) holds, with or without a tensor term.

D. Linear confinement

In this section we specify the momentum-dependent parts of the kernel and we discuss, in particular, how confinement is implemented in our CST model. In the literature there are several examples of confinement potentials. For instance, it is well known that the static potential in the quenched approximation of lattice QCD can be parametrized by a Cornell-type potential [39].

However the chiral limit is quite different from the quenched limit. In this paper we want to investigate how a linear scalar confinement can be made compatible with SχSB. Other Lorentz structures are possible, namely vector confinement, but here we choose scalar confinement as the most stringent case still able to hold the phenomenology of chiral symmetry.

To this end, we implement linear confinement in a relativistically generalized form of the momentum-dependent kernel functions V_{iR} in Eq. (22). The confinement part of the V_{iR}'s is denoted V_L, and its action on an arbitrary function ϕ of the off-shell quark momentum p, in the one-body CST-DE, is given by

$$\begin{aligned}\langle V_L\phi\rangle(p) = {} & \frac{1}{2}\int_k V_A(p,\hat{k})[\phi(\hat{k}) - \phi(\hat{p}_R)] \\ & + \frac{1}{2}\int_k V_A(p,-\hat{k})[\phi(-\hat{k}) - \phi(\hat{p}_R)],\end{aligned} \tag{26}$$

where

$$V_A(p,\hat{k}) = -h^2(p^2)h^2(m^2)\frac{8\pi\sigma}{(p-\hat{k})^4}, \tag{27}$$

and $\hat{k}$ is the on-shell quark momentum in the loop integral. The subtraction term, $\phi(\hat{p}_R)$, regularizes the singularities of

V_A at $(\hat{k}-\hat{p})^2=0$. The argument of the subtraction term is $\hat{p}_R=(E_{p_R},\mathbf{p}_R)$, where $\mathbf{p}_R=\mathbf{p}_R(p_0,\mathbf{p})$ are the values of $\mathbf{k}$ at which either $V_A(p,\hat{k})$ or $V_A(p,-\hat{k})$ become singular.

When applied to the wave function $\Psi(p_1,p_2)$ of a two-quark system depending on the quark momenta $p_1=p+P/2$ and $p_2=p-P/2$, the action of V_L is defined by

$$\begin{aligned}\langle V_L\Psi\rangle(p_1,p_2)=&\frac{1}{2}\int_k\left\{V_A\left(p,\hat{k}-\frac{P}{2}\right)[\Psi(\hat{k},\hat{k}-P)-\Psi(\hat{p}_{R1}^+,\hat{p}_{R1}^+-P)]+V_A\left(p,\hat{k}+\frac{P}{2}\right)[\Psi(\hat{k}+P,\hat{k})-\Psi(\hat{p}_{R2}^++P,\hat{p}_{R2}^+)]\right.\\&+V_A\left(p,-\hat{k}-\frac{P}{2}\right)[\Psi(-\hat{k},-\hat{k}-P)-\Psi(-\hat{p}_{R1}^-,-\hat{p}_{R1}^--P)]\\&\left.+V_A\left(p,-\hat{k}+\frac{P}{2}\right)[\Psi(-\hat{k}+P,-\hat{k})-\Psi(-\hat{p}_{R2}^-+P,-\hat{p}_{R2}^-)]\right\},\end{aligned}\tag{28}$$

where now

$$V_A(p,k)=-h(p_1^2)h(p_2^2)h(k_1^2)h(k_2^2)\frac{8\pi\sigma}{(p-k)^4},\tag{29}$$

with $k_1=k+P/2$, $k_2=k-P/2$, and $\mathbf{p}_{R1}^{\pm}$ and $\mathbf{p}_{R2}^{\pm}$ being the values of $\mathbf{k}$ at which $V_A(p,\pm\hat{k}-\frac{P}{2})$ and $V_A(p,\pm\hat{k}+\frac{P}{2})$ become singular, respectively. The CST wave functions where one quark is on shell are

$$\Psi(\hat{p}_1,p_2)=\Lambda(\hat{p}_1)\Gamma(\hat{p}_1,p_2)S(p_2),\tag{30}$$

$$\Psi(p_1,\hat{p}_2)=S(p_1)\Gamma(p_1,\hat{p}_2)\Lambda(\hat{p}_2).\tag{31}$$

The subtraction terms regularize both the *diagonal* singularities of V_A at $(\hat{k}-\hat{p})^2=0$, i.e., in channels where the same quark is on mass shell in the initial and intermediate states, and the *off-diagonal* singularities at $(\pm\hat{k}+P-\hat{p})^2=0$, which occur in channels with different quarks on mass shell in the initial and intermediate states. The subtraction also leads directly to the important relation

$$\langle V_L\rangle(p)=\int_k V_L(p,\hat{k})=0,\tag{32}$$

which is a relativistic generalization of the nonrelativistic $V_L(r=0)=0$.

Equation (32) allows the use of scalar, pseudoscalar, and tensor confining interactions in a way that is still consistent with chiral symmetry, because it makes it possible to satisfy Eq. (25). How this works in detail will be addressed shortly.

As a consequence of Eq. (32), the linear confinement V_L does not contribute to the scalar part of the self-energy $A(p^2)$ [which means that $A_L(p^2)=0$], nor to the pion equation in the chiral limit [22]. Therefore, a scalar component in the confinement potential is not necessarily inconsistent with chiral symmetry.

To discuss the implications of the AV-WTI on the kernel let us specify the Dirac structure of $\mathcal{V}_R$ as follows:

$$\begin{aligned}V_{SR}(p-k)&=\lambda_S V_{LR}(p-k),\\V_{PR}(p-k)&=\lambda_P V_{LR}(p-k),\\V_{VR}(p-k)&=\lambda_V V_{LR}(p-k)+\kappa_V V_{CR}(p-k),\\V_{AR}(p-k)&=\lambda_A V_{LR}(p-k)+\kappa_A V_{CR}(p-k),\\V_{TR}(p-k)&=\lambda_T V_{LR}(p-k).\end{aligned}\tag{33}$$

Here V_{LR} is the reduced version of V_L, and V_{CR} is a Lorentz invariant function representing the nonconfining part of the interquark interaction of Eq. (22). The weight parameters λ_i and κ_i are constants. For a pure vector–axial-vector kernel, with $\lambda_S=\lambda_P=\lambda_T=0$, Eq. (25) is trivially satisfied. However, a nontrivial realization is also possible. To obtain this, insert V_{SR}, V_{PR}, and V_{TR} of (33) into (25) and separate scalar and vector parts:

$$\begin{aligned}&\int_{k0}V_{SR}(p-k)\tilde{S}(k)+\int_{k0}V_{PR}(p-k)\tilde{S}(-k)\\&\quad+\frac{1}{2}\int_{k0}V_{TR}(p-k)\sigma^{\mu\nu}\tilde{S}(k)\sigma_{\mu\nu}\\&\propto(\lambda_S+\lambda_P+6\lambda_T)\int_k[V_{LR}(p-\hat{k})+V_{LR}(p+\hat{k})]\\&\quad+(\lambda_S-\lambda_P)\int_k\frac{\hat{k}}{m}[V_{LR}(p-\hat{k})-V_{LR}(p+\hat{k})].\end{aligned}\tag{34}$$

According to Eq. (32), the first integral vanishes because $\int_k V_L(p,\hat{k})=\int_k V_L(p,-\hat{k})=0$. For the second term to be zero we have to choose $\lambda_S=\lambda_P$, since the integral does not vanish. Note that λ_T is not constrained by Eq. (34) because the tensor part of the kernel does not contribute to the vector part of the self-energy. We conclude that a kernel that includes scalar linear confinement also requires an equal-weighted pseudoscalar counterpart, in order to satisfy the AV-WTI. Equation (32) implies that, in the chiral limit, only the nonconfining part of the kernel, $\mathcal{V}_C(p,k)=[\kappa_V(\gamma^\mu\otimes\gamma_\mu)+\kappa_A(\gamma^5\gamma^\mu\otimes\gamma^5\gamma_\mu)]V_C(p,k)$, contributes to

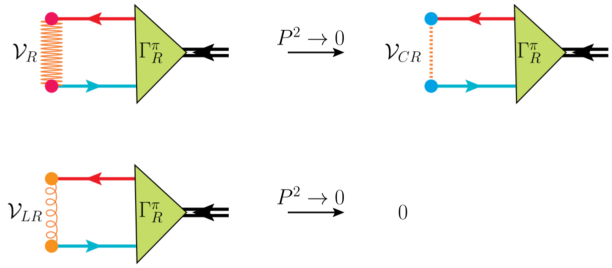

FIG. 3 (color online). In the chiral limit of vanishing pion mass only the nonconfining part of the kernel contributes to the pion CST equation. Each red or blue arrowed line denotes a dressed quark propagator. The light-blue and dark-yellow blobs denote the Dirac structures of $\mathcal{V}_{CR}$ and $\mathcal{V}_{LR}$, respectively.

the massless pion equation. This is diagrammatically depicted in Fig. 3 and was proven in Ref. [25].

With the AV-WTI-preserving CST choice $\lambda_S = \lambda_P$ the contributions of the scalar and the pseudoscalar parts of the linear confining kernel to the self-energy cancel exactly. Therefore, only the vector and axial-vector parts of the linear kernel contribute to the self-energy Σ, here denoted as Σ_L. However, as one moves away from the chiral limit the scalar, pseudoscalar, and tensor terms in the potential start to play a role.

Now, inserting Eq. (33) into Eq. (6) gives

$$\begin{aligned}\Sigma_L(p) &= -\mathrm{i}\int_{k0} V_{VR}(p-k)\gamma^\mu \tilde{S}(k)\gamma_\mu \\ &\quad -\mathrm{i}\int_{k0} V_{AR}(p-k)\gamma^5\gamma^\mu \tilde{S}(k)\gamma^5\gamma_\mu \\ &\propto 4(\lambda_V-\lambda_A)\int_k [V_{LR}(p-\hat{k})+V_{LR}(p+\hat{k})] \\ &\quad -2(\lambda_V+\lambda_A)\int_k \frac{\hat{\not{k}}}{m}[V_{LR}(p-\hat{k})-V_{LR}(p+\hat{k})].\end{aligned} \tag{35}$$

As in Eq. (34), the first integral vanishes because $\int_k V_L(p,\hat{k}) = \int_k V_L(p,-\hat{k}) = 0$. The second integral does not vanish and contributes to the self-energy, unless $\lambda_V = -\lambda_A$.

After this discussion of the general form of the interaction kernel, in the remainder of this paper we specialize to the particular case

$$\begin{aligned}\mathcal{V}_R(p-k) &= V_{LR}(p-k)\Big[\lambda_S(\mathbf{1}\otimes\mathbf{1})+\lambda_S(\gamma^5\otimes\gamma^5) \\ &\quad +\lambda_V(\gamma^\mu\otimes\gamma_\mu)+\lambda_A(\gamma^5\gamma^\mu\otimes\gamma^5\gamma_\mu) \\ &\quad +\frac{\lambda_T}{2}(\sigma^{\mu\nu}\otimes\sigma_{\mu\nu})\Big]+V_{CR}(p-k) \\ &\quad \times[\kappa_V(\gamma^\mu\otimes\gamma_\mu)+\kappa_A(\gamma^5\gamma^\mu\otimes\gamma^5\gamma_\mu)].\end{aligned} \tag{36}$$

E. The pion vertex function and the axial vertex in the chiral limit

Before we turn to π-π scattering, it is useful to consider the implications of the AV-WTI on the pion and on the axial vertex functions in the chiral limit.

1. Bare axial vertex

We start with the reduced bare axial vertex $\gamma_R^A(p',p)$ as parametrized in Eqs. (17)–(21). In the chiral limit of vanishing bare quark mass, $m_0 \to 0$, and vanishing vertex momentum, $P^\mu \to 0$, $f_A(p',p)$ remains finite whereas $g_A(p',p)$ vanishes, and thus the axial-vector vertex contracted with P^μ vanishes. For the remaining pseudoscalar part we have for the form factors in the limit $P^\mu \to 0$

$$f_P(p,p) = \frac{1}{h^2(p^2)} + \frac{2(m_0^2-p^2)}{h^3(p^2)}\frac{\mathrm{d}h(p^2)}{\mathrm{d}p^2} \tag{37}$$

and

$$g_P(p,p) = -\frac{8m_0^2}{h^3(p^2)}\frac{\mathrm{d}h(p^2)}{\mathrm{d}p^2}. \tag{38}$$

The derivative terms in $\gamma_R^A(p',p)$ of Eq. (17) cancel, and $\gamma_R^A(p,p)$ becomes

$$\gamma_R^A(p,p) = \frac{2m_0}{h^2(p^2)}\gamma^5, \tag{39}$$

as it should according to Eq. (16), and thus in the chiral limit

$$\lim_{\substack{m_0\to 0\\ p'\to p}} \gamma_R^A(p',p) = 0. \tag{40}$$

2. Dressed axial vertex

Because of Eq. (40), the CST-BS equation (12) for Γ_R^A becomes homogeneous in the chiral limit, and using the AV-WTI in the form of Eq. (11), this vertex function can be expressed directly in terms of the scalar mass function $A(p^2)$,

$$\Gamma_{R\chi}^A(p,p) = \gamma^5\frac{2A_\chi(p^2)}{h^2(p^2)}, \tag{41}$$

where A_χ is the chiral limit of A. Since a finite quark mass is generated by SχSB, A_χ is nonzero, and it is clear from Eq. (41) that $\Gamma_{R\chi}^A(p,p)$ must also be finite in this limit. Note that the pion produces poles in both Γ_R^5 and $\Gamma_R^{5\mu}$, with the corresponding residues constrained to cancel through the AV-WTI (for details, see, for instance, Ref. [32]). In Ref. [25], we found that the CST-BSE (1) for a massless pion becomes identical to the scalar part of the CST-DE (6) in the chiral limit, provided the interaction kernel satisfies condition (25). This implies, in particular, the relation

$$\Gamma^{\pi}_{R\chi}(p,p) = \gamma^5 G_0 Z_0 \frac{A_\chi(p^2)}{m_\chi h^2(p^2)} = \frac{G_0 Z_0}{2m_\chi}\Gamma^{A}_{R\chi}(p,p). \quad (42)$$

Here the constant G_0 is the inverse norm of the pion vertex function $\Gamma^{\pi}_{R\chi}$, calculated from the triangle diagram for the pion form factor at zero-momentum transfer and m_χ is the dressed quark mass, obtained by solving the equation $M_\chi(p^2 = m_\chi^2) = m_\chi$ with $m_0 = 0$ and the strong quark form factors normalized to $h(m_\chi^2) = 1$.

The next task is to use the AV-WTI to evaluate the π-π scattering amplitude at threshold in the chiral limit, with the kernel iterated to all orders, and to obtain the Adler zero, along the lines of Ref. [32].

IV. π-π SCATTERING

A. π-π scattering in impulse approximation

We start by calculating the π-π scattering amplitude in the impulse approximation, and we show that, in order to obtain the Adler zero, one has to go beyond impulse approximation.

The box diagram D_O (s-channel amplitude) of the full impulse contribution (sum of s, u, and t-channel amplitudes) to π-π scattering is depicted in Fig. 4. In the CST, it is proportional to [32]

$$\begin{aligned} D_O \propto -\mathrm{i}\int_{k0} \mathrm{tr}[&\bar{\Gamma}^{\pi}_{R}(k+P_1-P_4, k+P_1)\tilde{S}(k+P_1) \\ &\times \Gamma^{\pi}_{R}(k+P_1,k)\tilde{S}(k)\Gamma^{\pi}_{R}(k,k-P_2) \\ &\times \tilde{S}(k-P_2)\bar{\Gamma}^{\pi}_{R}(k-P_2,k-P_2+P_3) \\ &\times \tilde{S}(k+P_1-P_4)], \end{aligned} \quad (43)$$

where Γ^{π}_{R} is the reduced pion vertex function. In the chiral limit and in the pion rest frames ($P_i^\mu = 0$ where $i = 1, 2$ label the two incoming and $i = 3, 4$ the two outgoing pions) the pion vertex functions are given by Eq. (42), and therefore D_O becomes

$$\begin{aligned} D_{O\chi} &\propto -\mathrm{i}\int_{k0} \frac{A_\chi^4}{(1-B_\chi)^4(M_\chi^2-k^2)^4} \\ &\quad\times \mathrm{tr}[\gamma^5(M_\chi+k)\gamma^5(M_\chi+k)\gamma^0\gamma^{5\dagger}\gamma^0 \\ &\quad\times (M_\chi+k)\gamma^0\gamma^{5\dagger}\gamma^0(M_\chi+k)] \\ &= -\mathrm{i}\int_{k0}\frac{A_\chi^4}{(1-B_\chi)^4(M_\chi^2-k^2-\mathrm{i}\epsilon)^2}. \end{aligned} \quad (44)$$

This integral has 2 double poles at $k_0 = \pm\sqrt{m_\chi^2+\mathbf{k}^2} \mp \mathrm{i}\epsilon = \pm E_k \mp \mathrm{i}\epsilon$. Introducing the energy of the running mass, $\mathcal{E}_k = \sqrt{M_\chi^2+\mathbf{k}^2}$, and retaining only the residues of the propagator pole contributions, one obtains

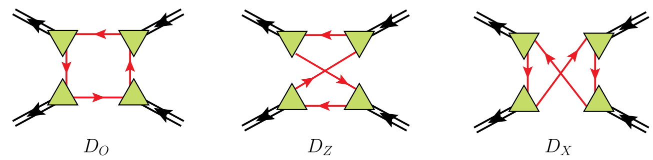

FIG. 4 (color online). The direct contributions to π-π scattering.

$$\begin{aligned} D_{O\chi} &\propto -\mathrm{i}\int_{k0}\frac{M_\chi^4}{(k_0-\mathcal{E}_k+\mathrm{i}\epsilon)^2(k_0+\mathcal{E}_k-\mathrm{i}\epsilon)^2} \\ &= \frac{1}{2}2\pi\int_k\left\{\left[\frac{4m_\chi^3 M'_{\chi 0}}{2E_k} - \frac{m_\chi^4}{4E_k^3}(1+2m_\chi M'_{\chi 0})\right]\right. \\ &\quad\left. - \left[-\frac{4m_\chi^3 M'_{\chi 0}}{2E_k} + \frac{m_\chi^4}{4E_k^3}(1-2m_\chi M'_{\chi 0})\right]\right\} \\ &= \pi\int_k\left[\frac{4m_\chi^3 M'_{\chi 0}}{E_k} - \frac{m_\chi^4}{2E_k^3}\right] \neq 0, \end{aligned} \quad (45)$$

where

$$M'_{\chi 0} \equiv \left.\frac{\mathrm{d}M_\chi(k^2)}{\mathrm{d}k^2}\right|_{k^2=m_\chi^2} = \frac{1}{2E_k}\left.\frac{\mathrm{d}M_\chi(k^2)}{\mathrm{d}k_0}\right|_{k^2=m_\chi^2}. \quad (46)$$

The two terms in (45) are nonzero, and they do not cancel. The same result is obtained for D_Z and D_X. One concludes that, in order to obtain the Adler zero from the amplitude in the chiral limit, one has to go beyond the impulse approximation. Therefore, the calculation of the quark-quark ladder sum to include intermediate-state interactions is unavoidable for crucial cancellations to occur. To achieve this, we extend the strategy of Refs. [31,32] to accommodate scalar, pseudoscalar, and tensor linear confinement in the CST formalism.

B. Prerequisites

1. Axial-vector Ward-Takahashi identity and the ladder sum

Because we are going to deal with diagrams which include a ladder sum in the intermediate state and at each vertex, it is useful to establish a Ward-Takahashi identity for the axial vertex when "sandwiched" between two ladder sums. In order to derive this identity, it is convenient to introduce some definitions and useful relations. First, we introduce the "unamputated" quark-antiquark scattering amplitude in the ladder approximation, $L(p'_1, p'_2; p_1, p_2)$. It includes the external propagators, two from the initial state and two from the final state (except for the inhomogeneous term, which has only two). Using a direct product representation, with $[\tilde{S}(k_1)\otimes\tilde{S}(k_2)] \equiv \tilde{S}_{\alpha\alpha'}(k_1)\tilde{S}_{\beta'\beta}(k_2)$, where $\alpha, \alpha'(\beta, \beta')$ are the Dirac indices for particle 1(2), so that, for example,

$$[\tilde{S}(k_1)\otimes\tilde{S}(k_2)]\Gamma(k_1,k_2)\equiv\tilde{S}_{\alpha\alpha'}(k_1)\tilde{S}_{\beta'\beta}(k_2)\Gamma_{\alpha'\beta'}(k_1,k_2)=[\tilde{S}(k_1)\Gamma(k_1,k_2)\tilde{S}(k_2)]_{\alpha\beta}, \tag{47}$$

the ladder sum (frequently referred to simply as the "ladder") is

$$\begin{aligned}L(p_1',p_2';p_1,p_2)&=-\mathrm{i}[\tilde{S}(p_1')\otimes\tilde{S}(p_2')](2\pi)^4\delta^4(p-p')+[\tilde{S}(p_1')\otimes\tilde{S}(p_2')]\mathrm{i}\int_{k0}\mathcal{V}_R(p'-k)L(k_1,k_2;p_1,p_2)\\&=-\mathrm{i}[\tilde{S}(p_1')\otimes\tilde{S}(p_2')](2\pi)^4\delta^4(p-p')+\mathrm{i}\int_{k0}L(p_1',p_2';k_1,k_2)\mathcal{V}_R(k-p)[\tilde{S}(p_1)\otimes\tilde{S}(p_2)],\end{aligned} \tag{48}$$

where $p_1^{(\prime)}=p^{(\prime)}+P^{(\prime)}/2$ and $p_2^{(\prime)}=p^{(\prime)}-P^{(\prime)}/2$, and the phases are as given in Ref. [27], with a factor of $-\mathrm{i}$ for each propagator, vertex function (*except* pseudoscalar or axial-vector vertices, which have no such factor), kernel, or scattering amplitude, an overall factor of i, and an additional factor of -1 for each closed fermion loop. This sum is diagrammatically depicted in Fig. 5.

It is shown in the Appendix how the insertion of the axial vertex into line 1 of an infinite ladder sum can be reduced using the Ward-Takahashi identity. The result is

$$\begin{aligned}\langle L|\Gamma_R^A|L\rangle&=\int_{k0}L(p_1',p_2';k_1',k_2)[\Gamma_R^A(k_1',k_1)\otimes\tilde{S}^{-1}(k_2)]L(k_1,k_2;p_1,p_2)\\&=-\mathrm{i}(\gamma^5\otimes\mathbf{1})L(p_1',p_2';p_1,p_2)-\mathrm{i}L(p_1',p_2';p_1,p_2)(\gamma^5\otimes\mathbf{1})\\&\quad+\mathrm{i}\int_{k0'}\int_{k0}L(p_1',p_2';k_1',k_2')[\mathcal{V}_R(k'-k)(\gamma^5\otimes\mathbf{1})+(\gamma^5\otimes\mathbf{1})\mathcal{V}_R(k'-k)]L(k_1,k_2;p_1,p_2).\end{aligned} \tag{49}$$

When the kernel $\mathcal{V}$ anticommutes with γ^5 [which is true for the vector and axial-vector pieces of the kernel in Eq. (36)] the last term vanishes [31,40]. The final result in this case was given in Refs. [31,32] and is depicted in Fig. 6. For the more general case when $\{\gamma^5,\mathcal{V}\}\neq 0$ the result is depicted in Fig. 7, where the last four diagrams correspond to the extension of the Ward-Takahashi identity of Fig. 6. Equation (49) will be used later.

Applying the ladder equation (48), we can rewrite the BSE (12) for the axial vertex Γ_R^A [31]. Using the direct product notation,

$$\begin{aligned}-\mathrm{i}[\tilde{S}(p_1)\otimes\tilde{S}(p_2)]\Gamma_R^A(p_1,p_2)&=-\mathrm{i}[\tilde{S}(p_1)\otimes\tilde{S}(p_2)]\gamma_R^A(p_1,p_2)+\int_{k0}[\tilde{S}(p_1)\otimes\tilde{S}(p_2)]\mathcal{V}_R(p-k)[\tilde{S}(k_1)\otimes\tilde{S}(k_2)]\gamma_R^A(k_1,k_2)\\&\quad+\mathrm{i}\int_{k0}[\tilde{S}(p_1)\otimes\tilde{S}(p_2)]\mathcal{V}_R(p-k)[\tilde{S}(k_1)\otimes\tilde{S}(k_2)]\\&\quad\times\int_{k0'}\mathcal{V}_R(k-k')[\tilde{S}(k_1')\otimes\tilde{S}(k_2')]\gamma_R^A(k_1',k_2')+\dots\\&=\int_{k0}L(p_1,p_2;k_1,k_2)\gamma_R^A(k_1,k_2).\end{aligned} \tag{50}$$

2. Spectral decomposition of the ladder sum

We apply the spectral decomposition of the ladder, assuming that it contains a bound-state pole at $P^2=m_\pi^2$, the pion pole. The ladder amplitude can then be related to the reduced bound-state vertex function for the pion as follows:

$$L(p_1',p_2';p_1,p_2)=[\tilde{S}(p_1')\otimes\tilde{S}(p_2')]\frac{\Gamma_R^\pi(p_1',p_2')\bar{\Gamma}_R^\pi(p_2,p_1)}{m_\pi^2-P^2-\mathrm{i}\epsilon}[\tilde{S}(p_1)\otimes\tilde{S}(p_2)]+\mathcal{R}(p_1',p_2';p_1,p_2), \tag{51}$$

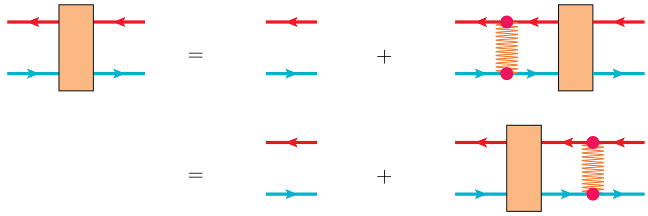

FIG. 5 (color online). The self-consistent equations for the unamputated quark-antiquark scattering amplitude, denoted by the orange box.

where $\mathcal{R}$ is the regular remainder at $P^2 = m_\pi^2$ which also includes the poles of all the other meson states. The only assumption we make about $\mathcal{R}$ is that none of its poles resides exactly at the pion mass, which is of course satisfied for any kernel that describes the meson spectrum and that is consistent with $S\chi$SB. Note that the sign of the pole term is positive because the pion is a pseudoscalar bound state (it would be negative for a scalar bound state), and that the separation between pole and nonpole terms is not unique away from the pole. Equation (51) is shown graphically in Fig. 8.

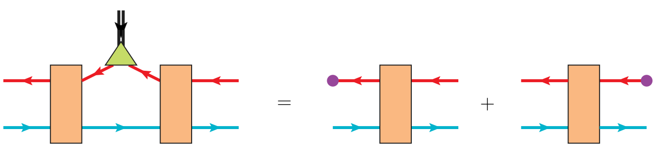

FIG. 6 (color online). Ward-Takahashi identity for the ladder of a kernel with $\{\mathcal{O}_i, \gamma^5\} = 0$. The purple blobs denote γ^5's.

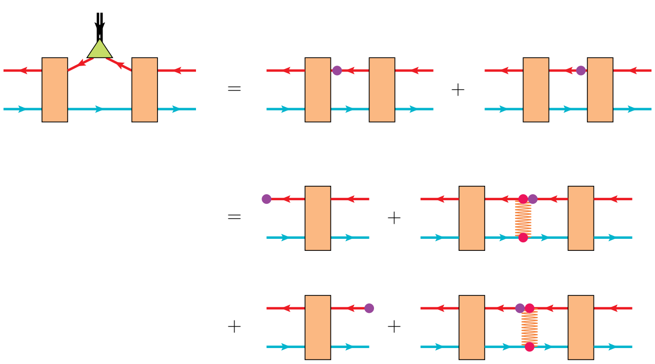

FIG. 7 (color online). By inserting the AV-WTI and ladder equation into the lhs of Eq. (49) one obtains the Ward-Takahashi identity for the ladder.

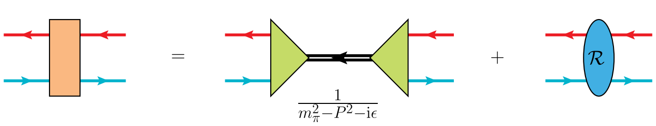

FIG. 8 (color online). Spectral decomposition of the ladder with the pion pole at m_π^2 explicitly displayed.

3. Relation for the off-shell pion vertex function

A useful relation for inserting a ladder at a pion vertex function is obtained from Eq. (51) by multiplying by i times the vertex function from the right and integrating over p. One obtains

$$
\begin{aligned}
&[\tilde{S}(p_1') \otimes \tilde{S}(p_2')]\Gamma_R^\pi(p_1', p_2') \\
&\quad = \frac{m_\pi^2 - P^2}{\mathcal{I}} \mathrm{i} \int_{p0} L(p_1', p_2'; p_1, p_2)\Gamma_R^\pi(p_1, p_2) \\
&\qquad - \frac{m_\pi^2 - P^2}{\mathcal{I}} \mathrm{i} \int_{p0} \mathcal{R}_\pi(p_1', p_2'; p_1, p_2)\Gamma_R^\pi(p_1, p_2),
\end{aligned}
\tag{52}
$$

where

$$
\mathcal{I} = \mathcal{I}(P) = \mathrm{i} \int_{k0} \mathrm{tr}\{\bar{\Gamma}_R^\pi(k_2, k_1)[\tilde{S}(k_1) \otimes \tilde{S}(k_2)]\Gamma_R^\pi(k_1, k_2)\}
\tag{53}
$$

and $\mathcal{R}_\pi$ is the part of $\mathcal{R}$ that couples to the pion channel. Since the integral of the second term on the rhs of Eq. (52) involving $\mathcal{R}_\pi$ has no poles at $P^2 = m_\pi^2$, this term can be dropped because at the end of the calculation we will only be interested in *on-shell* pion momenta P for which the factor $m_\pi^2 - P^2$ becomes zero. Alternatively, since the separation between the pion pole and nonpole residue $\mathcal{R}_\pi$ is not unique away from the pion pole, we may *choose* to set $\mathcal{R}_\pi = 0$, which *uniquely* defines the off-shell pion vertex function. We will adopt this point of view. Without the $\mathcal{R}_\pi$ term the off-shell extension of the pion vertex function is uniquely defined as the solution of

$$
\begin{aligned}
&[\tilde{S}(p_1') \otimes \tilde{S}(p_2')]\Gamma_R^\pi(p_1', p_2') \\
&\quad = \frac{m_\pi^2 - P^2}{\mathcal{I}} \mathrm{i} \int_{p0} L(p_1', p_2'; p_1, p_2)\Gamma_R^\pi(p_1, p_2).
\end{aligned}
\tag{54}
$$

Equation (54) effectively shows how one can add a ladder to—or remove it from—the pion vertex function (see Fig. 9).

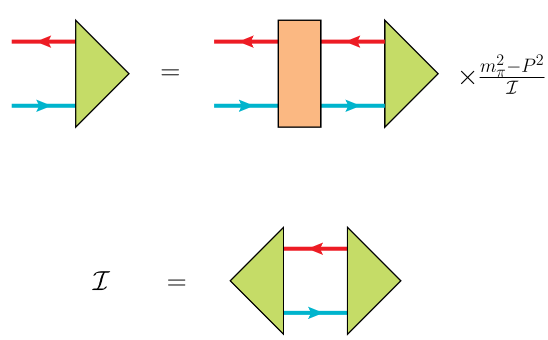

FIG. 9 (color online). Relation for the off-shell pion vertex function.

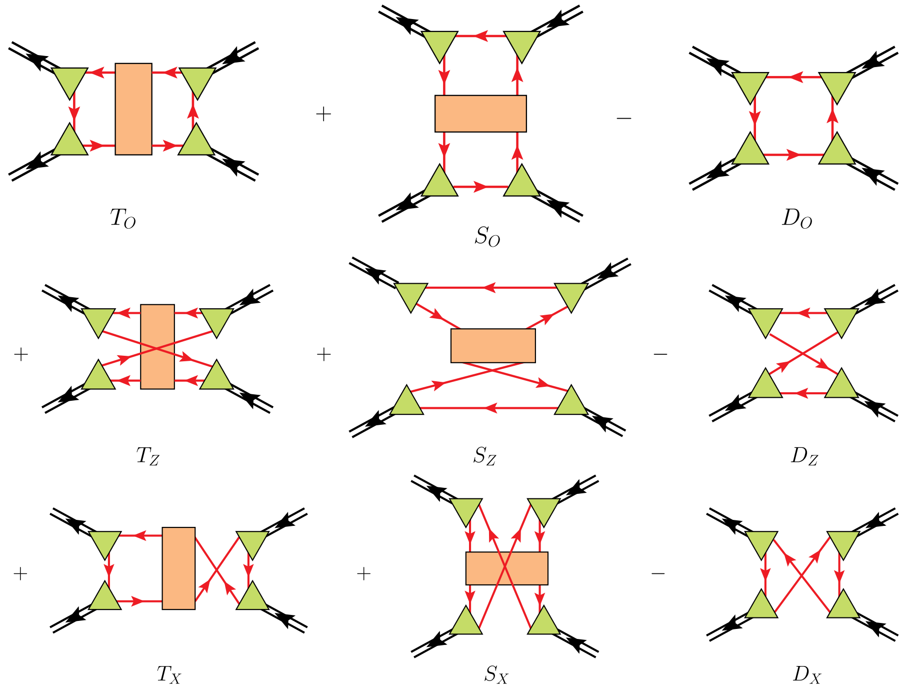

FIG. 10 (color online). Contributions to π-π scattering.

C. π-π scattering in the chiral limit: The Adler self-consistency zero

Now we are ready to calculate π-π scattering to all orders in the chiral limit. Our aim is to show that, in the chiral limit, the scattering amplitude vanishes. This is known as the Adler self-consistency zero [23]. Our derivation closely follows the one of Ref. [31].

There are three types of contributions, referred to as O, Z, and X diagrams, which are shown in the three rows of Fig. 10.

The D terms in each line, D_O, D_X, and D_Z, must be subtracted in order to avoid double counting of the direct contributions of Sec. IV A. We start our discussion by looking at the three diagrams of the first row (the O diagrams). We will show that, in the chiral limit, the sum of the three diagrams vanishes,

$$T_O + S_O - D_O \to 0. \tag{55}$$

Because of the similar topologies, the sums of the diagrams in the second and third row, respectively, also vanish.

We start with T_O. Remembering the minus sign for a closed fermion loop,

$$\begin{aligned} T_O = \int_{k0'}\int_{k0} \mathrm{tr}\{[\bar{\Gamma}^\pi_R(k'-P_3,k')\tilde{S}(k')\bar{\Gamma}^\pi_R(k',k'+P_4)] \\ \times L(k'+P_4,k'-P_3;k+P_1,k-P_2) \\ \times [\Gamma^\pi_R(k+P_1,k)\tilde{S}(k)\Gamma^\pi_R(k,k-P_2)]\}, \end{aligned} \tag{56}$$

with the ladder connecting incoming pions of momentum P_1, P_2 to outgoing pions with momentum P_3, P_4. Note that at this stage only the remainder term $\mathcal{R}$ from Eq. (51) contributes to the ladder L. This is because in Eq. (56) L is projected onto two pion vertex functions and therefore its pion pole term does not contribute (there is no $\pi \to 2\pi$ coupling by G-parity conservation).

In order to evaluate this diagram, we first consider the scattering when $P_2^2 \neq m_\pi^2$, and make use of the off-shell definition of the pion vertex function, Eq. (54), to insert another ladder into Eq. (56) by replacing $\Gamma^\pi_R(k,k-P_2)$ (this step is shown diagrammatically in the top panel of Fig. 11). This gives

$$\begin{aligned} T_O = \frac{m_\pi^2 - P_2^2}{\mathcal{I}(P_2)}\mathrm{i}\int_{k0'}\int_{k0}\int_{p0} \mathrm{tr}\{[\bar{\Gamma}^\pi_R(k'-P_3,k')\tilde{S}(k')\bar{\Gamma}^\pi_R(k',k'+P_4)]L(k'+P_4,k'-P_3;k+P_1,k-P_2) \\ \times [\Gamma^\pi_R(k+P_1,k)\tilde{S}^{-1}(k-P_2)L(k,k-P_2;p,p-P_2)\Gamma^\pi_R(p,p-P_2)]\}. \end{aligned} \tag{57}$$

Note that in this equation, the first ladder already present in Eq. (56) still does not have any pion pole contribution, while the second *inserted* ladder contains *only* pseudoscalar contributions, including the pion pole. Still, in anticipation of the next step, it is convenient to keep the notation general.

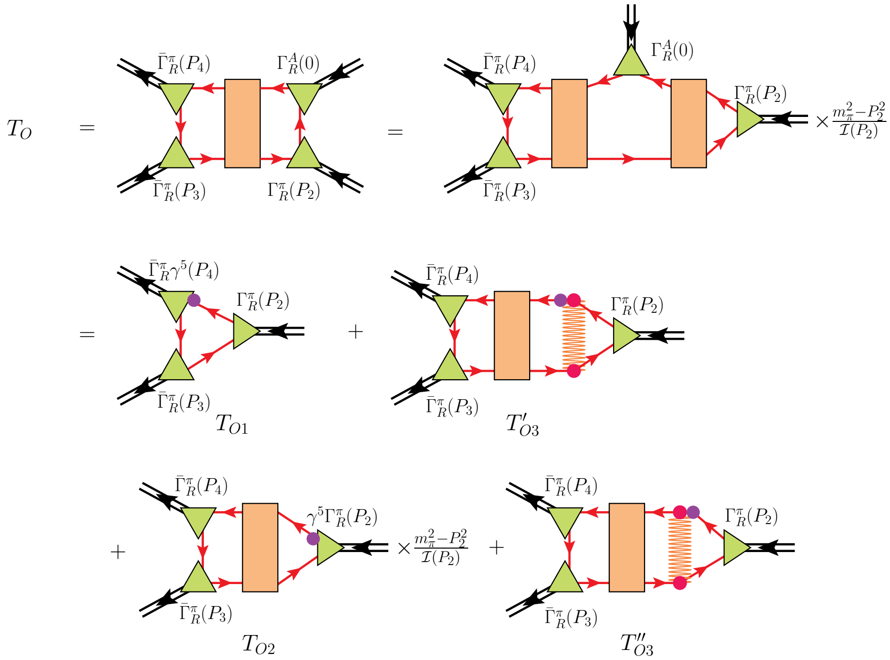

FIG. 11 (color online). Expansion of T_O in terms of T_{O1}, T_{O2}, T'_{O3}, and T''_{O3}. Here we use the shorthand notation $\Gamma(P)$, with P being the pion momentum. Notice the γ^5 matrix denoted by the purple blob that multiplies one of the pion vertex functions in T_{O1} and T_{O2}.

Next we let $P_1 \to 0$ (so that $P_2 = P_3 + P_4$), use (42) to replace $\Gamma^{\pi}_{R}(k,k)$ by $\Gamma^{A}_{R}(k,k)$, and then make use of the Ward-Takahashi identity (49) to replace the product of the two ladders. This generates four terms, all of which are further reduced using (51). They are depicted in the middle and bottom panels of Fig. 11 and given by

$$T_O = T_{O1} + T_{O2} + T'_{O3} + T''_{O3}, \tag{58}$$

$$\begin{aligned} T_{O1} &= \frac{G_0 Z_0 (m_\pi^2 - P_2^2)}{2m_\chi \mathcal{I}} \int_{k0'} \int_{p0} \mathrm{tr}\{[\bar{\Gamma}^{\pi}_{R}(k'-P_3,k')\tilde{S}(k')\bar{\Gamma}^{\pi}_{R}(k',k'+P_4)]\gamma^5 L(k'+P_4,k'-P_3;p,p-P_2)\Gamma^{\pi}_{R}(p,p-P_2)\} \\ &\to -\frac{G_0 Z_0}{2m_\chi} \mathrm{i} \int_{k0} \mathrm{tr}[\bar{\Gamma}^{\pi}_{R}(k-P_2,k-P_4)\tilde{S}(k-P_4)\bar{\Gamma}^{\pi}_{R}(k-P_4,k)\gamma^5 \tilde{S}(k)\Gamma^{\pi}_{R}(k,k-P_2)\tilde{S}(k-P_2)], \end{aligned} \tag{59}$$

$$\begin{aligned} T_{O2} &= \frac{G_0 Z_0 (m_\pi^2 - P_2^2)}{2m_\chi \mathcal{I}} \int_{k0'} \int_{p0} \mathrm{tr}\{[\bar{\Gamma}^{\pi}_{R}(k'-P_3,k')\tilde{S}(k')\bar{\Gamma}^{\pi}_{R}(k',k'+P_4)]L(k'+P_4,k'-P_3;p,p-P_2)\gamma^5\Gamma^{\pi}_{R}(p,p-P_2)\} \\ &\to -\frac{G_0 Z_0}{2m_\chi}\frac{\mathcal{I}'}{\mathcal{I}} \mathrm{i} \int_{k0'} \mathrm{tr}[\bar{\Gamma}^{\pi}_{R}(k'-P_3,k')\tilde{S}(k')\bar{\Gamma}^{\pi}_{R}(k',k'+P_4)\tilde{S}(k'+P_4)\Gamma^{\pi}_{R}(k'+P_4,k'-P_3)\tilde{S}(k'-P_3)], \end{aligned} \tag{60}$$

$$\begin{aligned} T_{O3} &= -\frac{G_0 Z_0 (m_\pi^2 - P_2^2)}{m_\chi \mathcal{I}} \int_{k0'} \int_{k0} \int_{p0'} \int_{p0} \mathrm{tr}\Big\{[\bar{\Gamma}^{\pi}_{R}(k'-P_3,k')\tilde{S}(k')\bar{\Gamma}^{\pi}_{R}(k',k'+P_4)]L(k'+P_4,k'-P_3;k,k-P_2) \\ &\quad \times V_{LR}(k-p')\Big[\lambda_S(\gamma^5\otimes\mathbf{1}+\mathbf{1}\otimes\gamma^5)+\frac{1}{2}\lambda_T(\gamma^5\sigma^{\mu\nu}\otimes\sigma_{\mu\nu})\Big]L(p',p'-P_2;p,p-P_2)\Gamma^{\pi}_{R}(p,p-P_2)\Big\} \\ &\to \frac{G_0 Z_0}{m_\chi} \mathrm{i} \int_{k0'} \int_{k0} \int_{p0'} \mathrm{tr}\Big\{[\bar{\Gamma}^{\pi}_{R}(k'-P_3,k')\tilde{S}(k')\bar{\Gamma}^{\pi}_{R}(k',k'+P_4)]L(k'+P_4,k'-P_3;k,k-P_2) \\ &\quad \times V_{LR}(k-p')\Big[\lambda_S(\gamma^5\otimes\mathbf{1}+\mathbf{1}\otimes\gamma^5)+\frac{1}{2}\lambda_T(\gamma^5\sigma^{\mu\nu}\otimes\sigma_{\mu\nu})\Big][\tilde{S}(p')\otimes\tilde{S}(p'-P_2)]\Gamma^{\pi}_{R}(p',p'-P_2)\Big\}, \end{aligned} \tag{61}$$

where $T_{O3} = T'_{O3} + T''_{O3}$, and in the second expression for T_{O1} we introduced $k = k' + P_4$, and

$$\mathcal{I}' = \mathcal{I}'(P) = \mathrm{i} \int_{k0} \mathrm{tr}[\bar{\Gamma}^{\pi}_{R}(k_2,k_1)[\tilde{S}(k_1)\gamma^5 \otimes \tilde{S}(k_2)]\Gamma^{\pi}_{R}(k_1,k_2)]. \tag{62}$$

Before proceeding further, it is useful to reflect on the physical content of these equations. The first line of each equation is the result from one of the contributions from the Ward-Takahashi identity (49). For example, Eq. (58) collapses, symbolically, $L_1\Gamma_R^A L_2 \to \gamma^5 L_3$ where, as already pointed out, L_1 [the first ladder in Eq. (57)] contained no pion channel (think of a ρ, for example), L_2 [the second ladder in Eq. (57)] contained the pion channel (take the π itself), and L_3 [the ladder in Eq. (58)] is general and could contain the pion pole. Physically, this contribution would then represent a $\rho\pi\pi$ transition collapsing to a $\gamma^5\pi$ coupling. Then, the second line in each equation shows how, because of the factor $m_\pi^2 - P_2^2$ from the insertion of L_2 multiplying the equation, only the pion pole term will survive the $P_2^2 \to m_\pi^2$ limit (remember that $\mathcal{R}$ has no pole at $P_2^2 = m_\pi^2$), reducing an initial ρ contribution (in this example) in L_1 to a box involving three pion vertex functions and one γ^5 (it is this additional γ^5 at one pion vertex that prevents this diagram from vanishing). This remarkable collapse of L_1 is a consequence of the Ward-Takahashi identity and the chiral limit.

While T_{O1} survives the chiral limit, the other terms vanish. The term $T_{O2} \to 0$ because $\Gamma^\pi_{R\chi} \propto \Gamma^A_{R\chi}$ and hence $\mathcal{I}' \to 0$, since it is the trace of an odd number of γ^5 matrices. Physically, it is a consequence of the fact that the pion does not couple to the scalar channel. The reduction of T_{O3}, which is proportional to the anticommutator of $\mathcal{O}_i$ and γ^5, uses the results from Eq. (A2) which show that only contributions from the scalar, pseudoscalar, and tensor parts of the linear confining kernel will contribute. However, because of the decoupling of the linear confinement kernel from the zero-mass pion equation discussed in Sec. III D, each of these contributions integrates to zero in the chiral limit, and therefore $T_{O3} \to 0$. The only contribution from T_O to survive in the chiral limit is the triangle contribution T_{O1}.

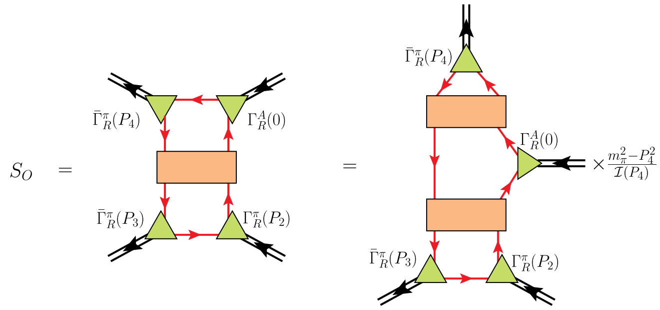

FIG. 12 (color online). The first step to reduce the second term S_O.

By considering a pion vertex with $P_4^2 \neq m_\pi^2$ the S_O diagrams can be computed in a similar way (the first step is shown in Fig. 12). The only term to survive is S_{O1}, the analogue of T_{O1}. Comparing Figs. 11 and 12 shows that the figures are identical if $P_4 \leftrightarrow -P_2$, since $P_1 = 0$ and $P_3 = P_2 - P_4$ is unchanged in both diagrams. Starting from this observation, S_{O1} can be transformed using the properties of the charge conjugation operation on the pion vertices, and the propagators

$$\begin{aligned}\mathcal{C}\Gamma_R^{\pi\intercal}(p_1,p_2)\mathcal{C}^{-1} &= \Gamma_R^\pi(-p_2,-p_1),\\ \mathcal{C}\tilde{S}^\intercal(p)\mathcal{C}^{-1} &= \tilde{S}(-p).\end{aligned} \tag{63}$$

This leads to

$$\begin{aligned}S_{O1} &= -\frac{G_0Z_0}{2m_\chi}\mathrm{i}\int_{k0}\mathrm{tr}[\bar\Gamma_R^\pi(k+P_4,k+P_2)\tilde{S}(k+P_2)\bar\Gamma_R^\pi(k+P_2,k)\gamma^5\tilde{S}(k)\Gamma_R^\pi(k,k+P_4)\tilde{S}(k+P_4)]\\ &= -\frac{G_0Z_0}{2m_\chi}\mathrm{i}\int_{k0}\mathrm{tr}[\Gamma_R^{\pi\intercal}(k+P_4,k+P_2)\tilde{S}^\intercal(k+P_4)\bar\Gamma_R^{\pi\intercal}(k,k+P_4)\tilde{S}^\intercal(k)(\gamma^5)^\intercal\bar\Gamma_R^{\pi\intercal}(k+P_2,k)\tilde{S}^\intercal(k+P_2)]\\ &= -\frac{G_0Z_0}{2m_\chi}\mathrm{i}\int_{k0}\mathrm{tr}[\Gamma_R^\pi(-k-P_2,-k-P_4)\tilde{S}(-k-P_4)\bar\Gamma_R^\pi(-k-P_4,-k)\tilde{S}(-k)\gamma^5\bar\Gamma_R^\pi(-k,-k-P_2)\tilde{S}(-k-P_2)]\\ &= -\frac{G_0Z_0}{2m_\chi}\mathrm{i}\int_{k0}\mathrm{tr}[\Gamma_R^\pi(k-P_2,k-P_4)\tilde{S}(k-P_4)\bar\Gamma_R^\pi(k-P_4,k)\tilde{S}(k)\gamma^5\bar\Gamma_R^\pi(k,k-P_2)\tilde{S}(k-P_2)],\end{aligned} \tag{64}$$

where, in the last line, we changed $k \to -k$, a transformation which also holds for the $k0$ prescription discussed above.

Next, the box diagram, for the special case when $P_1 = 0$, can be written

$$\begin{aligned}D_O &= -\mathrm{i}\int_{k0}\mathrm{tr}[\bar\Gamma_R^\pi(k-P_2,k-P_4)\tilde{S}(k-P_4)\bar\Gamma_R^\pi(k-P_4,k')\tilde{S}(k)\Gamma_R^\pi(k,k)\tilde{S}(k)\Gamma_R^\pi(k,k-P_2)\tilde{S}(k-P_2)]\\ &= -\frac{G_0Z_0}{2m_\chi}\mathrm{i}\int_{k0}\mathrm{tr}[\bar\Gamma_R^\pi(k-P_2,k-P_4)\tilde{S}(k-P_4)\bar\Gamma_R^\pi(k-P_4,k)(\gamma^5\tilde{S}(k)+\tilde{S}(k)\gamma^5)\Gamma_R^\pi(k,k-P_2)\tilde{S}(k-P_2)],\end{aligned} \tag{65}$$

where the second line first replaces the chiral limit of $\Gamma_R^\pi(k,k)$ by $\Gamma_{R\chi}^A$ using Eq. (42) and then uses the AV-WTI (11). From Eqs. (59), (64), and (65) we find that $T_{O1}+S_{O1}-D_O=0$, which completes the proof of Eq. (55).

Analogous considerations apply, of course, also to the Z and X diagrams. This constitutes the proof of the Adler self-consistency zero.

D. Gell-Mann–Oakes–Renner Relation

Although it is not directly related to π-π scattering, the Gell-Mann–Oakes–Renner relation is an important consequence of the AV-WTI. It is interesting to determine its form in the CST framework, because it involves the quark condensate given in terms of the dressed quark propagator, while in the CST we use damped dressed propagators.

To derive it, we extend the strategy of Ref. [31]. Starting with the CST-BSE for Γ_R^A, Eq. (50), inserting the spectral decomposition (51), and neglecting terms of order m_0 and P gives

$$\begin{aligned}\Gamma_R^A(p_1,p_2) &= [\tilde S(p_1)\otimes\tilde S(p_2)]^{-1}\mathrm{i}\int_{k0}L(p_1,p_2;k_1,k_2)\gamma_R^A(k_1,k_2)\\ &= \frac{\Gamma_R^\pi(p_1,p_2)}{m_\pi^2-P^2-\mathrm{i}\epsilon}\mathrm{i}\int_{k0}\mathrm{tr}[\tilde S(k_1)\bar\Gamma_R^\pi(k_1,k_2)\tilde S(k_2)\gamma_R^A(k_1,k_2)].\end{aligned} \tag{66}$$

Taking the $P^2\to 0$ limit of both sides, and using the relation (42) to cancel the common factor of $\Gamma_{R\chi}^A$ (where we neglect terms of order m_π and P in the difference between $\Gamma_{R\chi}^A$ and $\lim_{P^2\to 0}\Gamma_R^A$), gives the condition

$$1=\frac{G_0Z_0}{2m_\chi m_\pi^2}\mathrm{i}\int_{k0}\mathrm{tr}[\tilde S(k)\bar\Gamma_R^\pi(k,k)\tilde S(k)\gamma_R^A(k,k)]. \tag{67}$$

Next note that, in our model, the pion decay constant f_π is defined by [31]

$$\sqrt{2}f_\pi P^\mu=\mathrm{i}\int_{k0}\mathrm{tr}[\tilde S(k)\bar\Gamma_R^\pi(k,k)\tilde S(k)\gamma_R^{5\mu}(k,k)]. \tag{68}$$

Contracting (68) with P_μ and comparing it with Eqs. (67) and (17), we conclude that

$$\frac{f_\pi}{\sqrt{2}}=\frac{m_\chi}{G_0Z_0}. \tag{69}$$

Next, return to Eq. (67) and use Eq. (42) to replace Γ_R^π by $\Gamma_{R\chi}^A$, Eq. (39) to replace γ_R^A by γ^5, and (69) to replace G_0Z_0 by f_π, giving

$$\begin{aligned}f_\pi^2m_\pi^2 &= m_0\mathrm{i}\int_{k0}\mathrm{tr}[\tilde S(k)\bar\Gamma_{R\chi}^A(k,k)\tilde S(k)\gamma^5]\frac{1}{h^2(k)}\\ &= -m_0\mathrm{i}\int_{k0}\mathrm{tr}\{\tilde S(k)[\tilde S^{-1}(k)\gamma^5+\gamma^5\tilde S^{-1}(k)]\\ &\quad\times\tilde S(k)\gamma^5\}\frac{1}{h^2(k)}\\ &= -2m_0\mathrm{i}\int_{k0}\mathrm{tr}\,S(k),\end{aligned} \tag{70}$$

where we used the AV-WTI, Eq. (11), to replace $\bar\Gamma_{R\chi}^A$ and $\bar\gamma^5=-\gamma^5$. Notice that the dependence on the strong quark form factors has canceled. Since the quark condensate is $\langle\bar qq\rangle\equiv\mathrm{i}\ \mathrm{tr}\int_k S(k)$, the Gell-Mann–Oakes–Renner relation follows:

$$f_\pi^2m_\pi^2=-2m_0\langle\bar qq\rangle. \tag{71}$$

V. SUMMARY AND CONCLUSIONS

This work describes the application of the CST to a dynamical quark model of π-π scattering. More generally, we have found that it is possible to preserve the essential AV-WTI even in the presence of a linear confining interaction with scalar and pseudoscalar components, provided only that these components have equal weight. (No restriction is placed on the strength of any vector, axial-vector, or tensor components of the confining interaction, nor on the vector or axial-vector components of any other type of interaction.) With a kernel with these limitations, the AV-WTI is satisfied and we show that, as a consequence, the Adler zero in the π-π scattering amplitude emerges automatically. This feature allows the CST model to be applied to both heavy and light quark systems.

While some of these results are shared by many other models with vector or axial-vector kernels that anticommute with γ^5, away from the chiral limit our linear confining interaction, if it has scalar, pseudoscalar, or tensor components, will produce contributions to the π-π scattering lengths not present in the famous Weinberg result [41]. We have not yet investigated how big these contributions might be—all that we know at present is that they must vanish in the chiral limit. Comparison of predictions for these effects with experimental data, together with the contributions of the confining interaction to the meson spectrum, will constrain the strength and spin structure of the confining interaction and will be a subject for future work.

A feature of our model is that strong quark form factors are used simultaneously (i) to describe the physical effects of overlapping exchange interactions that go beyond the rainbow approximation, and (ii) to provide a covariant regularization scheme.

It remains to be seen whether a scalar potential in the intermediate-quark-mass range could be thought of as a coherent superposition of vector gluons, but if that is so, the preservation of the AV-WTI requires that it must be accompanied by a pseudoscalar exchange. This is another topic for future study.

ACKNOWLEDGMENTS

This work received financial support from Fundação para a Ciência e a Tecnologia (FCT) under Grants No. PTDC/FIS/113940/2009 and No. CFTP-FCT (PEst-OE/FIS/U/0777/2013). The research leading to these results has received funding from the European Community's Seventh Framework Programme FP7/2007-2013 under Grant Agreement No. 283286. This work was also partially supported by Jefferson Science Associates, LLC, under U.S. DOE Contract No. DE-AC05-06OR23177. All diagrams have been drawn with JaxoDraw, Ref. [42].

APPENDIX

The identity (49) is proven as follows. We apply the AV-WTI of Eq. (11) (represented in Fig. 1) on the lhs of Eq. (49), and then use the self-consistent equations for the ladder sum, Eq. (48) represented in Fig. 5, to obtain four terms:

$$\begin{aligned}\langle L|\Gamma_R^A|L\rangle &= \int_{k0} L(p_1', p_2'; k_1', k_2)[\Gamma_R^A(k_1', k_1) \otimes \tilde{S}^{-1}(k_2)]L(k_1, k_2; p_1, p_2)\\ &= \int_{k0} L(p_1', p_2'; k_1', k_2)\{[\tilde{S}^{-1}(k_1')\gamma^5 + \gamma^5\tilde{S}^{-1}(k_1)] \otimes \tilde{S}^{-1}(k_2)\}L(k_1, k_2; p_1, p_2)\\ &= -\mathrm{i}(\gamma^5 \otimes \mathbf{1})L(p_1', p_2'; p_1, p_2) - \mathrm{i}\, L(p_1', p_2'; p_1, p_2)(\gamma^5 \otimes \mathbf{1})\\ &\quad + \mathrm{i}\int_{k0'}\int_{k0} L(p_1', p_2'; k_1', k_2')[\mathcal{V}_R(k'-k)(\gamma^5 \otimes \mathbf{1}) + (\gamma^5 \otimes \mathbf{1})\mathcal{V}_R(k'-k)]L(k_1, k_2; p_1, p_2). \end{aligned} \tag{A1}$$

All four terms of the rhs are depicted in Fig. 7. The two terms with the kernel (which is a sum of operators $\mathcal{O}_i$) are proportional to the anticommutator $\{\gamma^5, \mathcal{O}_i\}$. For vector and axial-vector spin structures, they vanish, leaving only the two terms of the rhs of Fig. 6. For the scalar, pseudoscalar, and tensor structures of the linear confining part of the kernel, $\{\gamma^5, \mathcal{O}_i\} \neq 0$, and therefore we must keep these terms in all calculations. Specifically, for the kernel of Eq. (36), Eq. (A1) becomes

$$\begin{aligned}\langle L|\Gamma_R^A|L\rangle &= -\mathrm{i}(\gamma^5 \otimes \mathbf{1})L(p_1', p_2'; p_1, p_2) - \mathrm{i}\, L(p_1', p_2'; p_1, p_2)(\gamma^5 \otimes \mathbf{1})\\ &\quad + 2\mathrm{i}\int_{k0'}\int_{k0} L(p_1', p_2'; k_1', k_2')\left[\lambda_S(\gamma^5 \otimes \mathbf{1} + \mathbf{1} \otimes \gamma^5) + \frac{1}{2}\lambda_T(\gamma^5\sigma^{\mu\nu} \otimes \sigma_{\mu\nu})\right]V_{LR}(k'-k)L(k_1, k_2; p_1, p_2). \end{aligned} \tag{A2}$$

Notice the factor of 2 since $\{\gamma^5, \mathcal{O}_i\} = 2\gamma^5\mathcal{O}_i$ for $i = S$, P, and T.

[1] S. Godfrey and N. Isgur, Phys. Rev. D **32**, 189 (1985).
[2] E. Eichten, K. Gottfried, T. Kinoshita, J. Kogut, K. D. Lane, and T.-M. Yan, Phys. Rev. Lett. **34**, 369 (1975).
[3] E. Eichten, K. Gottfried, T. Kinoshita, K. D. Lane, and T.-M. Yan, Phys. Rev. D **17**, 3090 (1978).
[4] J. L. Richardson, Phys. Lett. **82B**, 272 (1979).
[5] R. G. Edwards, N. Mathur, D. G. Richards, and S. J. Wallace, Phys. Rev. D **87**, 054506 (2013).
[6] P. Guo, J. J. Dudek, R. G. Edwards, and A. P. Szczepaniak, Phys. Rev. D **88**, 014501 (2013).
[7] S. J. Brodsky, H.-C. Pauli, and S. S. Pinsky, Phys. Rep. **301**, 299 (1998).
[8] J. Carbonell, B. Desplanques, V. A. Karmanov, and J.-F. Mathiot, Phys. Rep. **300**, 215 (1998).
[9] J. H. O. Sales, T. Frederico, B. V. Carlson, and P. U. Sauer, Phys. Rev. C **61**, 044003 (2000).
[10] I. Bars and M. B. Green, Phys. Rev. D **17**, 537 (1978).
[11] A. Amer, A. Le Yaouanc, L. Oliver, O. Pene, and J.-C. Raynal, Phys. Rev. Lett. **50**, 87 (1983).
[12] A. Le Yaouanc, L. Oliver, O. Pene, and J. C. Raynal, Phys. Lett. **134B**, 249 (1984).
[13] P. J. de A. Bicudo and J. E. F. T. Ribeiro, Phys. Rev. D **42**, 1611 (1990).
[14] P. J. de A. Bicudo and J. E. F. T. Ribeiro, Phys. Rev. D **42**, 1625 (1990).
[15] P. J. de A. Bicudo and J. E. F. T. Ribeiro, Phys. Rev. D **42**, 1635 (1990).
[16] A. V. Nefediev and J. E. F. T. Ribeiro, Phys. Rev. D **70**, 094020 (2004).
[17] R. Alkofer and L. von Smekal, Phys. Rep. **353**, 281 (2001).
[18] P. Maris and C. D. Roberts, Int. J. Mod. Phys. E **12**, 297 (2003).

[19] C. S. Fischer, J. Phys. G **32**, R253 (2006).

[20] E. Rojas, J. P. B. C. de Melo, B. El-Bennich, O. Oliveira, and T. Frederico, J. High Energy Phys. 10 (2013) 193.

[21] E. P. Biernat, F. Gross, M. T. Peña, and A. Stadler, Phys. Rev. D **89**, 016006 (2014).

[22] F. Gross and J. Milana, Phys. Rev. D **45**, 969 (1992).

[23] S. L. Adler, Phys. Rev. **137**, B1022 (1965).

[24] C. Savkli and F. Gross, Phys. Rev. C **63**, 035208 (2001).

[25] E. P. Biernat, F. Gross, M. T. Peña, and A. Stadler, Phys. Rev. D **89**, 016005 (2014).

[26] E. E. Salpeter and H. A. Bethe, Phys. Rev. **84**, 1232 (1951).

[27] F. Gross, *Relativistic Quantum Mechanics and Field Theory*, revised ed. (Wiley, New York, 1999).

[28] F. Gross, Phys. Rev. **186**, 1448 (1969).

[29] F. Gross and J. Milana, Phys. Rev. D **43**, 2401 (1991).

[30] S. L. Adler, Phys. Rev. **177**, 2426 (1969).

[31] P. Bicudo, Phys. Rev. C **67**, 035201 (2003).

[32] P. Bicudo, S. Cotanch, F. Llanes-Estrada, P. Maris, E. Ribeiro, and A. Szczepaniak, Phys. Rev. D **65**, 076008 (2002).

[33] F. Gross and D. O. Riska, Phys. Rev. C **36**, 1928 (1987).

[34] F. Gross and Y. Surya, Phys. Rev. C **47**, 703 (1993).

[35] Y. Surya and F. Gross, Phys. Rev. C **53**, 2422 (1996).

[36] S. L. Adler and A. C. Davis, Nucl. Phys. **B244**, 469 (1984).

[37] P. Maris and C. D. Roberts, Phys. Rev. C **56**, 3369 (1997).

[38] J. E. Villate, D-S. Liu, J. E. Ribeiro, and P. J. de A. Bicudo, Phys. Rev. D **47**, 1145 (1993).

[39] C. R. Allton *et al.*, Phys. Rev. D **65**, 054502 (2002).

[40] P. J. de A. Bicudo, Phys. Rev. C **60**, 035209 (1999).

[41] S. Weinberg, Phys. Rev. Lett. **17**, 616 (1966).

[42] D. Binosi and L. Theussl, Comput. Phys. Commun. **161**, 76 (2004).